Geosynthetics-reinforced embankment on engineered slope

S. Cuomo, P. Gambardella
University of Salerno, Italy (scuomo@unisa.it)

L. Frigo
Geosintex s.r.l., Sandrigo, Italy

F. Cosma
Edilfloor s.p.a., Sandrigo, Italy

ABSTRACT: Marginally stable slopes are a problematic context for anthropogenic excavations and artificial embankments. This topic is dealt with in this paper aimed at providing quantitative estimates of both soil deformations and displacements of the ground surface induced by the renewal works of an important highway in Southern Italy. Particularly, the original slope was firstly excavated and then reshaped, also adding a line of Concrete Piles (CP). As major work, a high embankment was built and reinforced through 12 lines of PVC coated polyester geogrids. Apart from a multilayered stratigraphy, the study area was also characterized by a landslide deposit of weak clayely soils located just beneath the toe of the Georeinforced Reinforced Embankment (GRE). Therefore, this paper investigates the role of the Concrete Piles towards the overall performance of the GRE-CP system, varying either the length or the diameter of the piles. FEM (Finite Element Method) seepage steady-state analysis and stress-strain analysis were performed assuming an elastic-plastic contact law at the interface between the piles and soils, and a Mohr-Coulomb contact law at the interface between the geogrids and the embankment soil. As main results, the paper outlines four principal scenarios for slope deformation and embankment performance, related to different types of piles used for the slope reinforcement.

Keywords: geogrid, slope, landslide, pile, displacement.

1 INTRODUCTION

Artificial embankments such as Geosynthetics-Reinforced Embankments (GRE) may suffer excessive settlements when lying on weak soils or marginally stable slopes. This latter case is analyzed in the paper with special reference to a case history of Southern Italy. During the renewal of a South-North principal highway, additional preventive construction works were needed inside an area where weak clayely soils exist. Moreover, in the same district previous landslide events had already caused damage and threats for the highway (Guida et al., 2008). First, the slope was engineered through the installation of Concrete Pile (CP), and then the GRE was constructed using PVC coated polyester geogrid. Indeed, slope stability can be increased by modifying the ground surface geometry, through superficial or deep drainage, using soil improvement techniques, installing continuous or discrete retaining structures such as walls or piles. The first remedy leads to a reduction of the driving forces for failure; the other measures tend instead to an increase of the resisting forces. Vertical piles have been successfully used in many situations to either stabilize slopes or improve slope stability, and numer-

ous methods exist for the analysis of piled slopes. Novel advanced design procedures based on displacement analysis have been also proposed (Galli and di Prisco, 2013). Whereas, former analyses of global and internal displacements of GER have been proposed by Cuomo et al. (2013) and Xue et al. (2014) among others.

The paper provides a quite comprehensive stress-strain analysis to outline the efficacy of the CP in order to reduce global displacements and internal deformations of the GRE. While the seepage flow beneath the GRE is analyzed under simplified assumption of steady state condition, the construction sequence of the GRE is accurately reproduced and attention has been posed to relevant mechanical issues like interface between soil and geogrids or concrete.

2 CASE STUDY

The area under investigation is located in Southern Italy, corresponding to a working area for the renewal and widening of the Italian A3 National Highway at Sirino-Lagonegro site (data courtesy of SIS S.p.c.a, ANAS s.p.a. and Geosintex s.r.l.). It is worth mentioning that areas beside to the highways were involved in past landslides (Guida et al., 2008) due to the presence of quite superficial weak clayley soils. This was an important issue to correctly design the geosynthetics-reinforced embankment. Indeed, reinforcement works were required also for the soils where the embankment was built upon. However, different solutions could be adopted even within the same class of intervention, such as large diameter concrete piles.

In the paper, the slope cross section of figure 1 was used as reference for computation. It is composed of inclined layers of four main soils, which are from the top to the bottom UG0, UG5a, UG2b and UG8. UG0 soils are mainly silty sands; UG2b includes silts and clays while UG5a is clayey silt with sand and gravel, whereas UG8 is fractured carbonate bedrock. Based on the results of boreholes, SPT and pressiometers tests, all the lithotypes were appropriately characterized to assess the mechanical parameters later used for geomechanical analysis.

Figure 1 outlines that the embankment under investigation is composed of two scarps: the lower scarp is 7.80 m high, sloping 2:1 at the front, and reinforced with 12 lines of geogrids made of PVC coated polyester, while the upper scarp is 6 m high, with inclination 33° to the horizontal and it is unreinforced. Specifically, in the lower reinforced scarp three types of geosynthetics were used, from the bottom: 2 lines of geogrids with maximum tensile strength equal to 80 kN/m at the base (Edilgrid 80/30), 6 lines of geogrids with maximum tensile strength equal to 55 kN/m (Edilgrid 55/30) and 4 lines of geogrids with maximum tensile

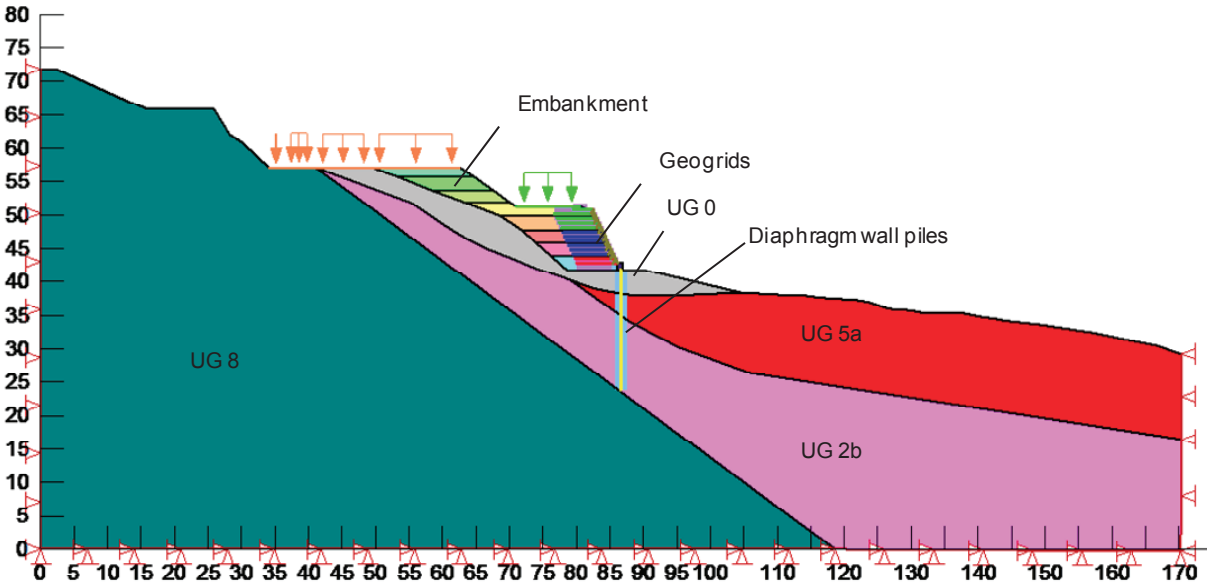

Figure 1: Slope section under investigation

strength equal to 35 kN/m (Edilgrid 35/20) at the uppermost portion of the scarp. Figure 1 also shows the construction sequence of the embankment by layers of about 0.65 m each. The external load applied at the top of the embankment above both the scarps was equal to 20kPa.

3 GEOMECHANICAL MODELLING

3.1 *Methods and input data*

The geomechanical modelling was based on Finite Element Method (FEM) analyses of the artificial embankment taking into account both the real complex stratigraphy of the site and the presence of a draining diaphragm wall made of non-contiguous bored concrete piles. The modeling consisted in: i) seepage analysis inside the soils beneath the artificial embankment, and ii) analysis of the stress-strain response of both the embankment and base soils.

Seepage analysis was performed through the commercial FEM code SEEP/W (Geoslope, 2005) only referring to base soils, being the embankment made of very coarse materials and equipped with drainage systems at the bottom contact with base soils.

Stress-strain analysis was conducted using the commercial FEM code SIGMA/W (Geoslope, 2005), assuming a purely elastic material model for concrete, a simple elastic-plastic constitutive mechanical model for soils and geogrids, and considering the existence of different mechanical properties of soil at the interface with geogrids and concrete pile diaphragm wall. Particularly, the geogrids were schematized as elastic "bar" elements, resistant to tensile stress up to an ultimate strength while not bearing bending moment. The geometry of geogrids was that typical of "wrap around" technique. At the front of the scarp, the steel metallic framework was simulated as elastic "bar" element (EA=2340 kN/m). The diaphragm wall was schematized as elastic "beam" element capable to support axial compression/tensile force and bending moments and made of concrete (C25/30, Rck30). At the top of the piles (i.e. at the base of the lower scarp), also the presence of a transversal concrete beam (H=1.0 m and B=0.8 m) was included in the numerical model, assuming an elastic behavior (γ=25 kN/m^3, E=32000 MPa, ν=0.49). Table 1 provides the mechanical properties of the materials.

For both analyses, an unstructured mesh of triangular elements not larger than 0.4 meters was adopted with mesh refinement around the geogrid lines (Fig. 2).

The scenarios considered for the analysis were four, different only for the presence and

Table 1. Material properties

	γ_{tot} (kN/m^3)	c' (kPa)	φ' (°)	ν (-)	E (MPa)	ψ (°)
UG0	18	2	33	0.33	75	10
UG2b	18	20	32	0.33	100	10
UG5a	18	7	14	0.33	15	14
UG8	24	600	34	0.29	1000	10
Embankment soil	18	2	33	0.33	75	10
*Material at Geogrid-Soil Interface	0	2	26	0.33	75	0
**Material at Beam-Soils Interface	0	2	14	0.45	65	0

Notes:
* T_n=20 kN/m or 30 kN/m for Edilgrid 35/20 or Edilgrid 55/30 and Edilgrid 80/30, respectively; EA= 450 kN/m or 600 kN/m or 850 kN/m for Edilgrid 35/20, Edilgrid 55/30 or Edilgrid 80/30, respectively.
** EI= 182000 kN/m^2/m or 575300 kN/m^2/m or 575300 kN/m^2/m for piles of scenario "2", "3" or "4", respectively.

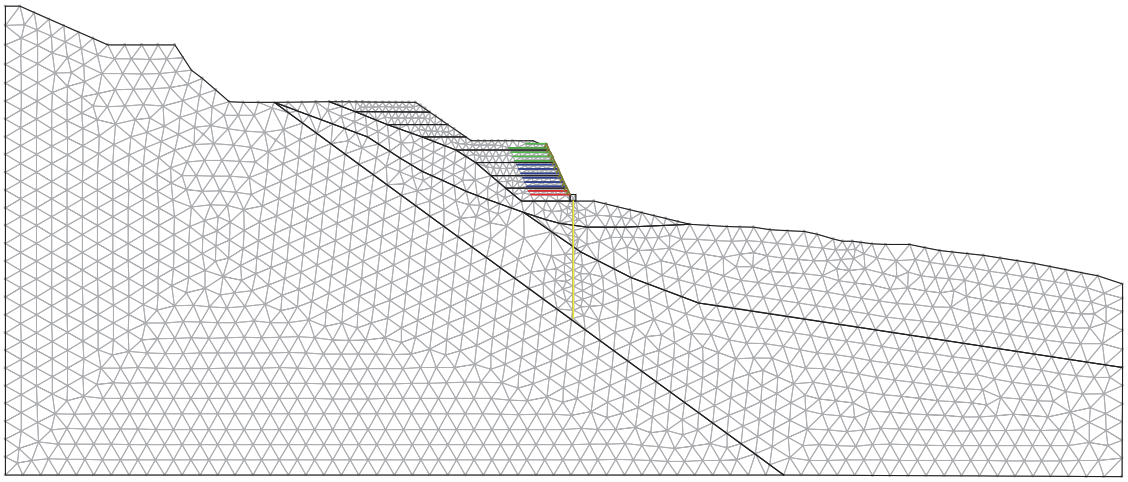

Figure 2: Spatial discretization for FEM analyses

dimensions of the concrete piles. Particularly, the natural slope without any reinforcement beneath the artificial embankment was labeled as scenario "1". The scenario "2" consisted of the longest piles (L=18 m) with the smallest diameters herein considered (D=0.6 m).

Relatively short piles (L=9 m) with the largest diameters (D=0.8 m) were considered in the so-called scenario "3". Finally, and intermediate case was the scenario "4", with long piles (L=18 m) and large pile diameter (D=0.8 m). In all the scenarios of reinforced slope, the centre to centre distance of piles was assumed equal to 1.1 m. Significant differences were expected for those scenarios in terms of displacements and deformations induced by the construction of the artificial embankment on the slope once differently engineered with piles.

3.2 *Simplified seepage analysis*

The simplified assumption of steady-state condition was made in relation to: the presence of fine-grained soils beneath the embankment; draining features of the diaphragm wall; relatively slow construction velocity for the embankment; and almost constant values of the total head (h=z+ p_w /γ_w, with z defined as the elevation of the ground, p_w as pore water pressure and γ_w as unit weight of water) measured at both the boundaries of the computational domain of Figure 2. Under these assumptions the solution of the Laplace governing equation is dependent only on the ratios of saturated conductivity of soils. In the following analyses, any difference in saturated conductivity for the present soils was not considered.

The steady-state pore water pressures (p_w) were computed with reference to different hydraulic boundary conditions. The bottom boundary was assumed impermeable. A constant total head condition was imposed at both the lateral boundaries. Along the ground surface of the slope beneath the artificial embankment a nil flux was imposed with the maximum pore water pressure not exceeding zero. Pore water pressures (p_w) were not computed but considered nil inside the whole embankment as it is made of very coarse material and with drainage systems at the contact with underneath soils. Finally, in correspondence to the draining diaphragm wall none of specific hydraulic conditions was applied, thus assuming that water can freely filtrate between non-contiguous concrete piles and beneath the whole diaphragm. Doing so, for the different scenarios of piles (longer or shorter, thicker or thinner) there isn't any difference for the computed pore water pressures.

Figure 3 shows the results of such simplified analysis for the scenario "2", which is identical to those obtained for the other scenarios. The computed pore water pressure contour lines are inclined to the horizontal direction, quasi-linear and almost equally-spaced. This means that a quasi-1D seepage flow was simulated within the slope. Correspondingly, above the computed piezometric line (i.e. p_w=0), negative pore water pressures were calculated which have a linear trend along the vertical. It is worth noting that at the vertical section corresponding to the wall diaphragm the computed piezometric line is almost located at upper

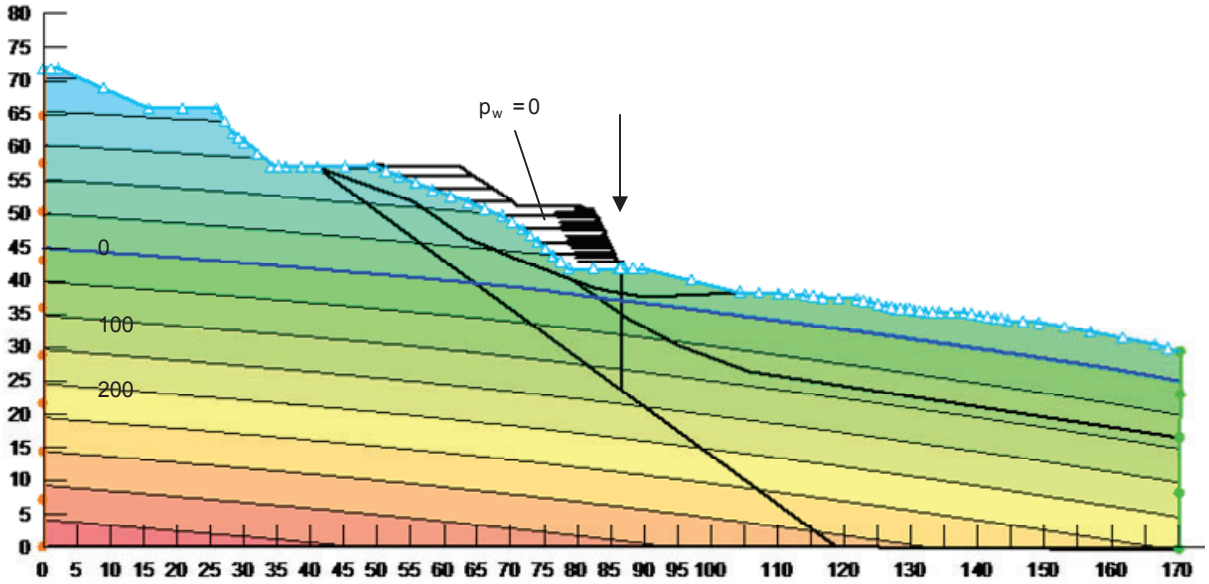

Figure 3: Pore water pressure contour lines

contact of UG5a soil with UG0, at a depth of about 6 m from the base of the embankment. Positive pore water pressures are attained within the weak UG5 soil and high values in the UG2b soil. Such a spatial distribution of pore water pressures represents a burdensome condition for the embankment to be added to the other two negative site-specific conditions that are the sloping base ground surface and the presence of weak soils.

3.3 *Stress-strain analyses*

The behavior of artificial embankment and underneath engineered slope was investigated in the framework of a multi-step analysis. First, a stress-strain analysis was performed in drained condition, assuming as input data the self-weight of soils and the steady-state pore water pressures computed in the sect. 2.2. Then, the time-sequence of the embankment construction was modeled simulating the construction of 8 soil layers reinforced through 12 lines of geogrids at the lower 2:1 sloping scarp while without any reinforcement at the upper 33° sloping upper scarp.

In all of the analyses, the horizontal displacements were assumed equal to zero at the lateral boundaries; whereas, the bottom boundary was assumed as completely fixed.

A simple non-associated elastic perfectly plastic Drucker-Prager (DP) constitutive model was assumed for all the soils, with the material properties reported in Table 1.

An important issue was related to the interface between different materials. The geogrid-soil interface (at both top and bottom sides) was modeled as an elastic-plastic DP material, schematized thorugh two arrays – 0.1 m thick – of elements at each side. The material was assumed as weightless, with the elastic parameters and cohesion equal to those of the confining soil (labeled as “Embankment Soil” in Tab. 1), while the effective friction angle – tan(φ’) – was assumed as 0.8 times that of confining soils, and with nil dilatancy. The beam-soils interface was modelled similarly to the previous case, with the only peculiarity related to the fact that this interface interacts with three different soils (UG0, UG5a, and UG2b). Thus, the shear strength parameters were derived from those of the weakest soil interacting with the beam.

The results of the stress-strain analysis for the scenario “1” outline that the maximum vertical displacement beneath the embankment is higher than 3 cm at the lower scarp. In the soil base layer of the embankment (UG0), vertical displacements are about 2 cm and, much importantly, the displacements computed are higher than 1 cm for the weak soil (UG5a).

Scenario “2” corresponds to a maximum computed vertical displacement similar to the previous case, while the displacements at the zone immediately downslope the artificial scarp

are much lower than for previous the case (about 5 mm in both UG0 and UG5a, instead of 1.5 cm and 1 cm, respectively, as in the previous case). It is significant that this kind of engineering solution for slope reinforcement is able to limit the displacements downslope the diaphragm wall while not reducing the maximum vertical displacement beneath the embank-

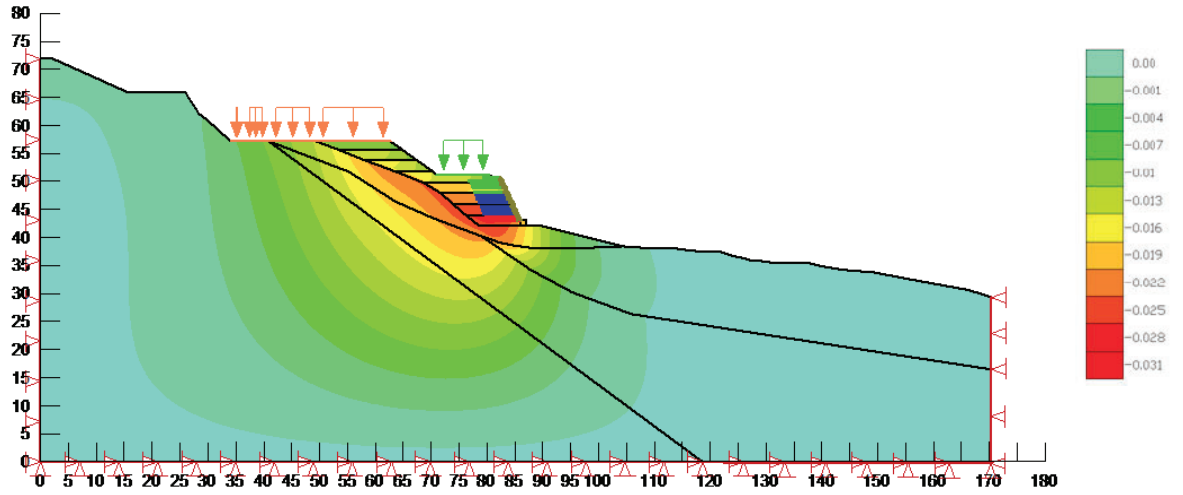

Figure 4: Vertical displacements for scenario 1 (unreinforced base slope)

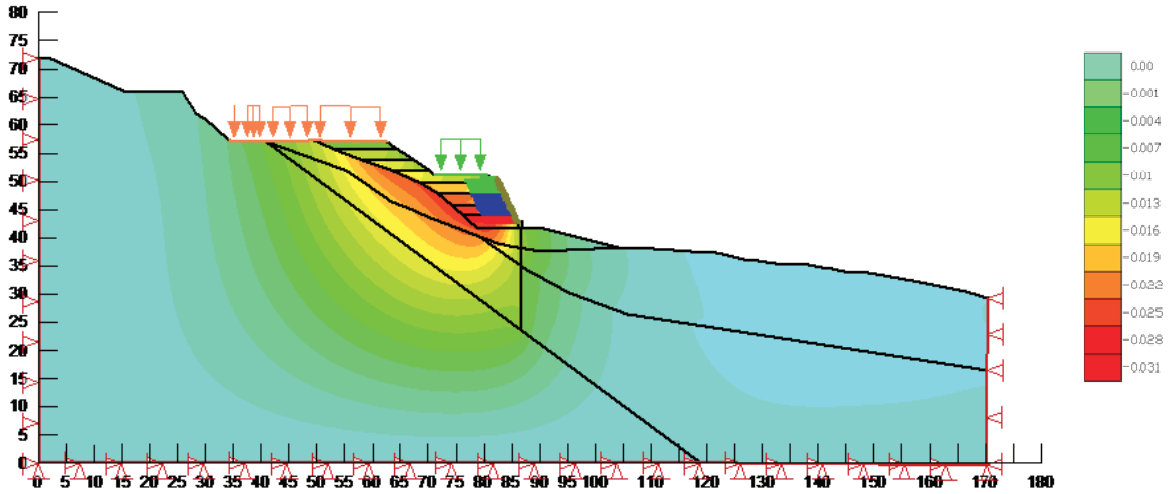

Figure 5: Vertical displacements for scenarios 2 (engineered slope with piles L=18 m, D=0.6 m).

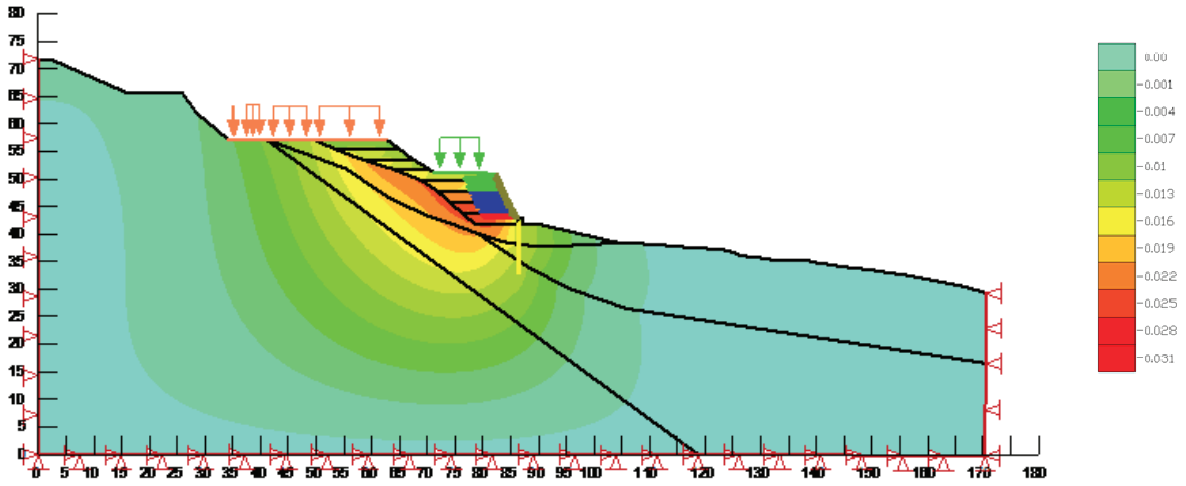

Figure 6: Vertical displacements for scenarios 3 (engineered slope with piles L=9 m, D=0.8 m)

ment. Such kind of performance is related to the features of the diaphragm (long and relatively thin). Thus the wall works like internal constraint to lateral (almost horizontal) deformations, which are then responsible for vertical deformations downslope the embankment.

Scenario "3" refers to "opposite-strategy" solution using shorter but stiffer piles than scenario "2". This means that piles overpass the base soil layer (UG0), the weak soil (UG5a) and limitedly the lower more resistant soil layer (UG2b). The positive effect of such intervention is evident for the base soil (UG0) and weak soil (UG5b) located downslope the wall, with a maximum vertical displacement quite similar to the previous pile-based slope reinforcement scenario "2". The higher stiffness of the wall plays a relevant role in the case under investigation. It is worth noting that the inertia momentum *EI* is proportional to the diaphragm thickness cubed.

Scenario "4" combines the best features of piles considered in the previous solutions, i.e. piles are long 18 m (almost reaching the contact between UG2b and bedrock), and 0.8 m thick. Such a stiff concrete work acts as a constraint for the whole slope with a twofold effect. First, down slope the embankment, the vertical displacements are reduced at the minimum amount among those computed. However, beneath the embankment, the maximum displacement rises from about 3.0 cm to 3.5 cm. Indeed, this latter effect is not surprising as the diaphragm wall, as long and stiff it is, can significantly reduce the soil volume interacting with the artificial embankment. This is a drawback one should be prepared to tackle. In the specific case history, the layer of weak soil UG5a has very limited thickness upslope the wall and it is thicker downslope. Thus, the performance of such a wall in such a case is appreciable.

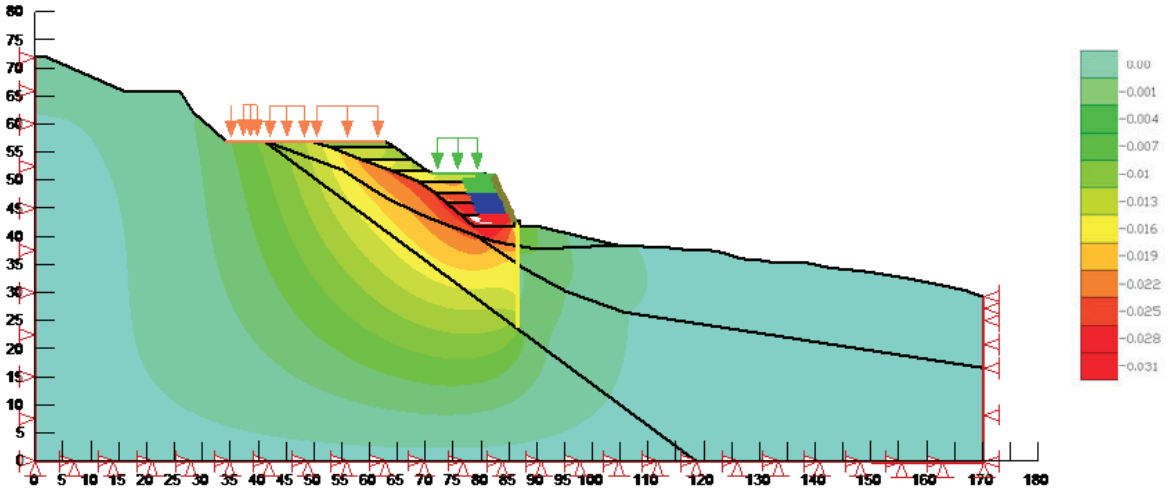

Figure 7: Vertical displacements for scenarios 4 (engineered slope with piles L=18 m, D=0.8 m)

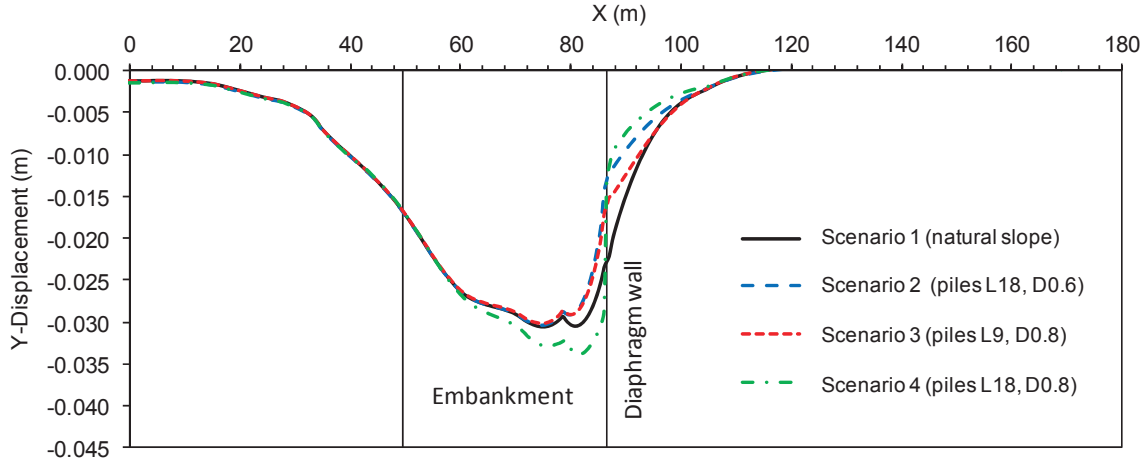

Figure 8: Vertical displacements of the ground surface beneath the embankment and along the slope

Aimed to provide a comparison among the above mentioned scenarios, figure 8 shows the plot of the computed vertical displacements along the former ground surface before construction, corresponding to the contact between embankment and slope after GRE construction. While not comprehensive, this comparison allows outlining the general differences of the three analyzed interventions. The more the vertical displacements are reduced downslope the diaphragm the more the displacements are increased below the embankment (scenario "4").

This type of slope response is much appreciable in the specific case history under investigation, as the weak layer is mostly located downslope the wall (Fig. 7). In general, the reinforcement of the slope would produce an increase of the vertical displacements below the embankment, contrarily to the main goal of the slope reinforcement. In this light, the scenarios "2" and "3" could be generally recommended for general cases of deep layers of weak soils. Some differences can be also outlined, because in the scenario "2" the piles diaphragm is long enough to reduce the vertical displacements induced by the embankment construction (Fig. 5). However, also a piles diaphragm stiff enough is capable to achieve the same effect (Fig. 6). Therefore, such a comparison outlines that both design options are reasonable, being the final choice also related to other issues, among which those related to construction costs and times.

As further analysis of the different behavior of slope, once differently engineered, it is worth computing the horizontal displacements at the vertical section corresponding to the concrete pile diaphragm with confining soils. In the case of unreinforced slope, horizontal displacements along the vertical are quite irregular (Fig. 9). This is because of the presence of so different soils (UG0 up to 3 m below the ground surface, UG5a at 3-7 m depth, and UG2b below), being UG0 and UG2b quite stiffer than the intermediate soil layer UG5a. This irregular trend of horizontal displacements along the vertical is modified for all the engineered slope solutions. This is a first remarkable effect of the pile diaphragm. Secondly, it can be observed that the length of piles plays a major role (Fig. 9), since the plots of scenarios "2" and "4" (i.e. long piles) are quite similar and globally corresponding to lower displacement for the weak intermediate layer UG5a. More surprisingly, the solution of scenario "3" is even more effective into reducing the horizontal displacements of the layer UG5a. This is easily explainable considering that the diaphragm pile is here stiff enough to inhibit the soil displacements where undesired, while allowing soil deformations where they are more acceptable, i.e. in the better soil UG2b located below the weak soil.

Thus, it is interesting noting that different performance assessments are possible for the analyzed interventions based on different, sometimes contrasting, requirements asked to the slope reinforcement intervention. In fact, an issue is the global reduction of vertical dis-

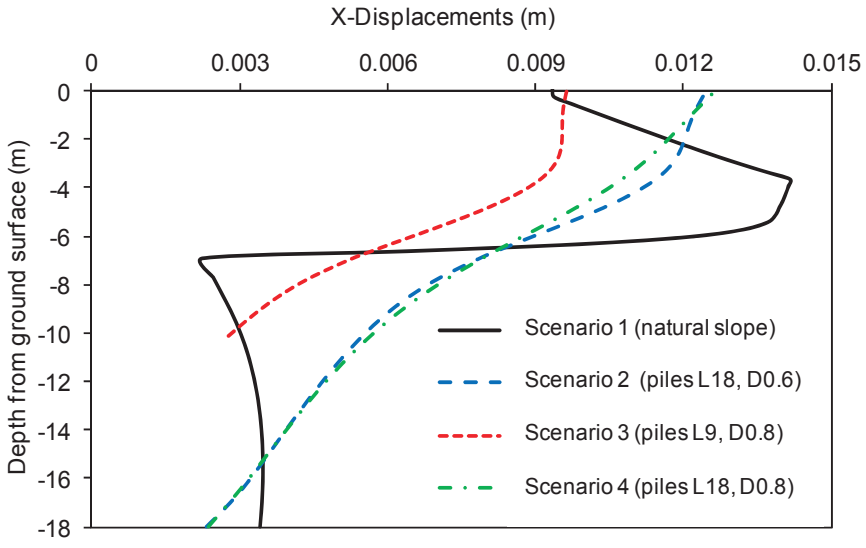

Figure 9: Horizontal displacements at the vertical section corresponding to the diaphragm wall

placements in the artificial embankment and in the slope beneath. This was discussed with contouring images of Figs. 4-7. Another design requirement could be related to the specific limitation of the vertical displacements at the ground surface, as discussed with reference to Fig. 8. In addition, the limitation of the horizontal displacements at the section where the diaphragm is constructed may represent another design requirement, as commented for Fig. 9. As additional insight, it is worth noting that the construction of an artificial reinforcement work may also have drawbacks, like concentration of displacements in a portion of the slope.

4 CONCLUSIONS

The paper dealt with a marginally stable slope also made of deep weak soil layer where an artificial Geosynthetics-Reinforced Embankment (GRE) was constructed, being interested to provide quantitative estimates of both soil deformations and displacements of the ground surface and at weak deep soil. Particularly, the original multilayered soils slope was firstly excavated and then re-shaped; also adding a line of Concrete Piles (CP) at the base of a high embankment, reinforced through 12 lines of PVC coated polyester geogrids.

After a simplified FEM (Finite Element Method) seepage analysis, a stress-strain analysis was performed assuming an elastic-plastic contact law at the interface between the piles and soils, and a Mohr-Coulomb contact law at the interface between the geogrids and the embankment soil.

As main result, the paper outlines four principal scenarios for the slope deformation and embankment performance, related to different types of piles used for the slope stabilization. It is interesting noting that different performance assessments are possible for the analyzed interventions based on different, sometimes contrasting, requirements asked to the slope reinforcement intervention such as: global or local reduction of vertical displacements, other than the reduction of the horizontal displacements at the section where the diaphragm is constructed. These issues could be also complemented to assessment of costs and times of all the possible solutions within a robust design procedure. Thus, the analyses proposed in the paper could provide a contribution towards a proper selection of the intervention for slope reinforcement as preventive work to GRE construction.

5 REFERENCES

Cuomo S., Frigo L., Tedesco C. (2013). Modelling the displacements of geosynthetics reinforced geostructures. Proceedings of the International Symposium on Design and Practice of Geosynthetic-Reinforced Soil Structures, Bologna, 14-16 October 2013. ISBN: 978-1-60595-108-9, pp. 1-10

Galli A., di Prisco C. (2013). Displacement-based design procedure for slope-stabilizing piles. Canadian Geotechnical Journal, 50, 41-53, DOI: 10.1139/cgj-2012-0104.

Guida, D., Pelfini, M., & Santilli, M. (2008). Geomorphological and dendrochronological analyses of a complex landslide in the Southern Apennines. Geografiska Annaler: Series A, Physical Geography, 90(3), 211-226.

Xue, J. F., Chen, J. F., Liu, J. X., Shi, Z. M. (2014). Instability of a geogrid reinforced soil wall on thick soft Shanghai clay with prefabricated vertical drains: A case study. Geotextiles and Geomembranes, 42(4), 302-311.

ACKNOWLEDGMENTS

The Authors would like to thank the companies SIS S.c.p.a., ANAS s.p.a. and Geosintex s.r.l. which, according to their own roles and responsibilities, provided the in-situ data and design information of the reinforced embankment of the Italian A3 National Highway (at Lagonegro site) which were fundamental to develop the numerical analyses reported in the paper.